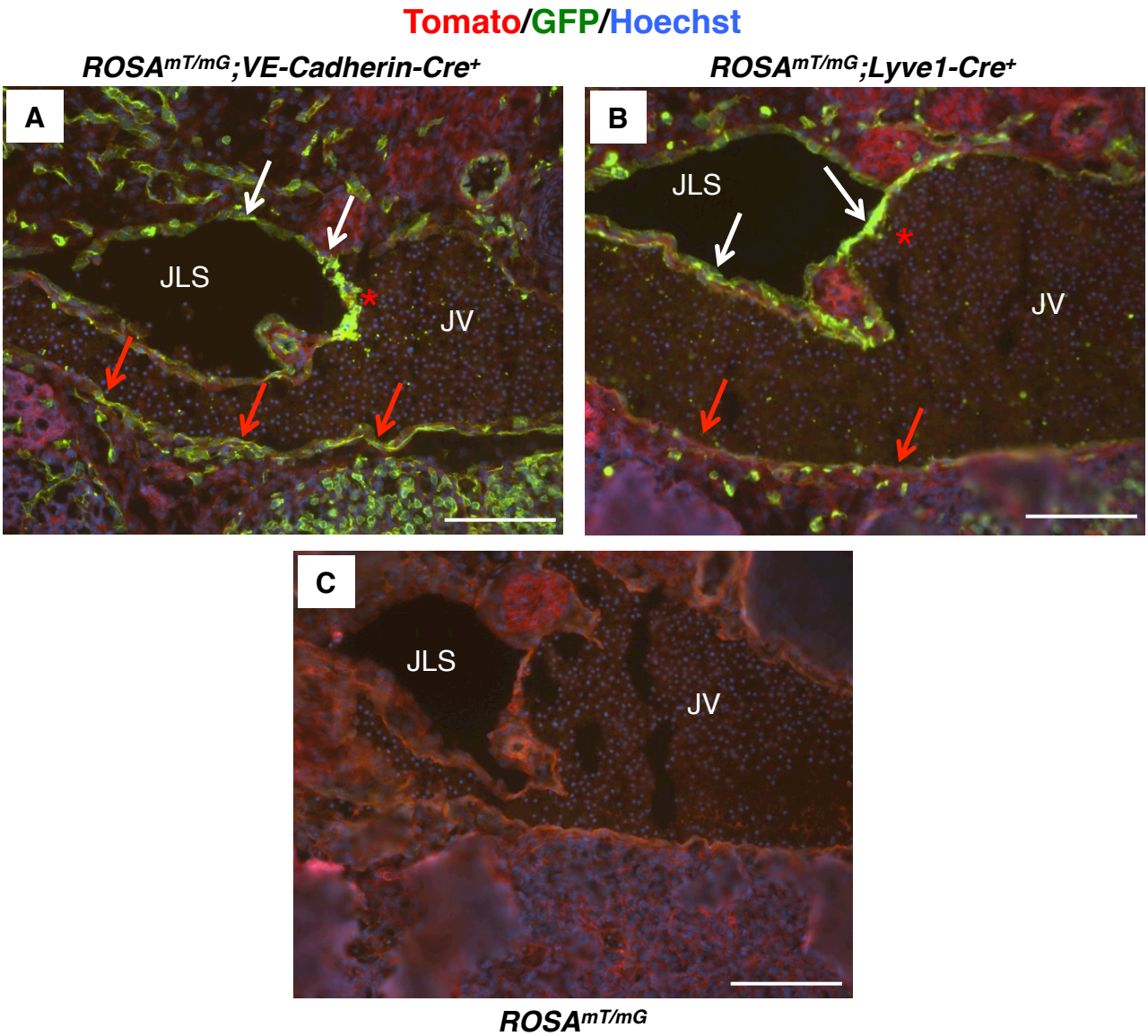

Supplemental Figure 1. *VE-Cadherin-Cre* and *Lyve1-Cre* activity. A double-fluorescent Cre reporter mouse (*ROSA*$^{mT/mG}$) was used to assess Cre recombinase activity. Membrane Tomato (mT; red) marks cells with no Cre activity; membrane GFP (mG; green) marks cells with Cre activity. **A)** *ROSA*$^{mT/mG}$*;VE-Cadherin-Cre*$^{+}$ embryos dissected at E14.5 showed robust Cre activity on both blood vessels (red arrows) and lymphatic vessels (white arrows). **B)** *ROSA*$^{mT/mG}$*;Lyve1-Cre*$^{+}$ embryos dissected at E14.5 showed robust Cre activity on lymphatic vessels (white arrows) but little activity on blood vessels (red arrows). **C)** E14.5 Cre-negative embryos (*ROSA*$^{mT/mG}$) showed no background GFP expression in either blood or lymphatic vessels. The asterisk (*) indicates sites of LVV development. n=3 embryos per genotype. Scale bars: 100µm. JLS=jugular lymph sac, JV=jugular vein.

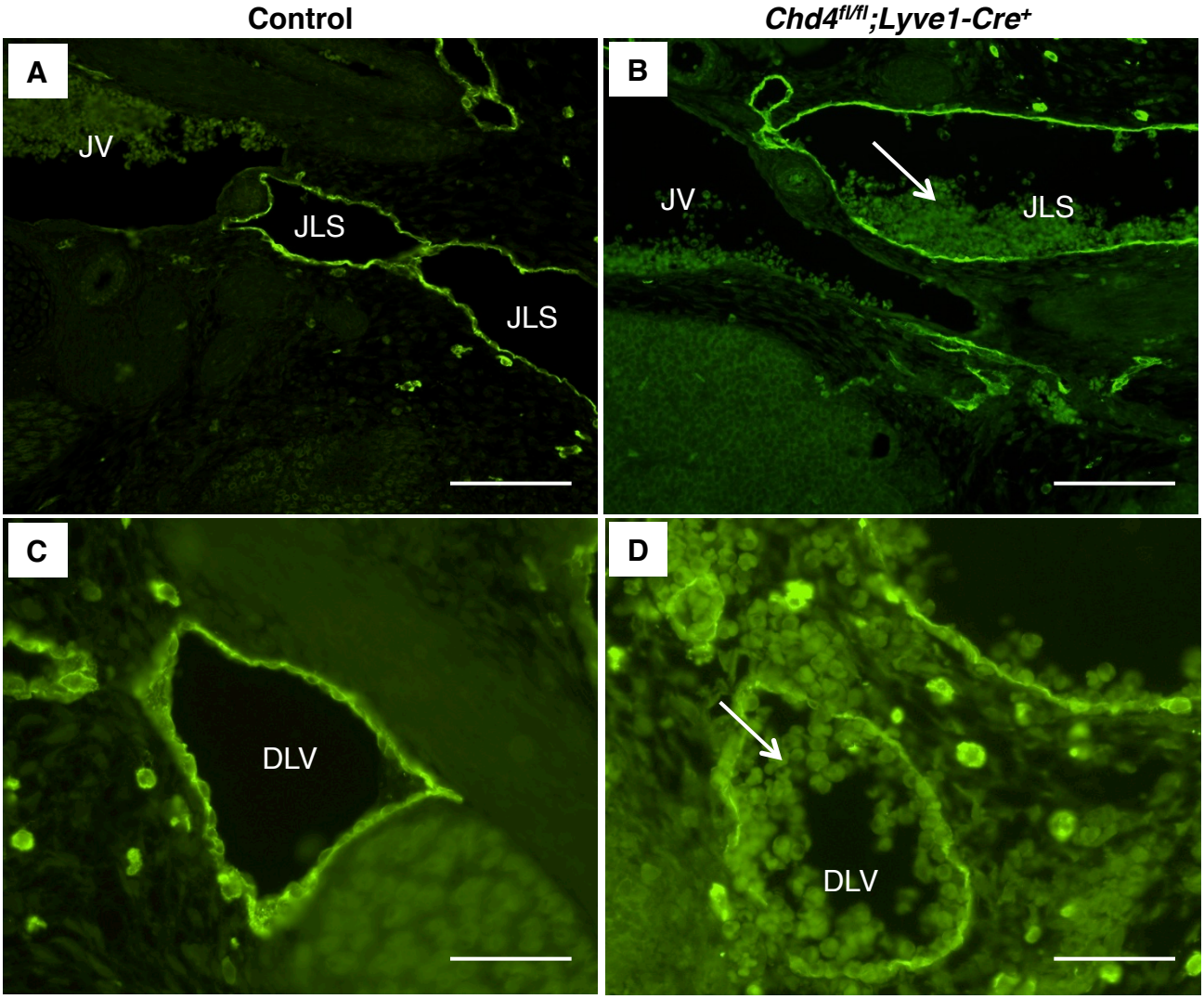

Supplemental Figure 2. LYVE1 is comparably expressed in jugular lymph sacs and dermal lymphatics of control and *Chd4$^{fl/fl}$;Lyve1-Cre^{+}* embryos. Sections from E14.5 control **(A and C)** and *Chd4$^{fl/fl}$;Lyve1-Cre^{+}* **(B and D)** embryos were immunostained for LYVE1 (green) to assess its expression in LECs. Expression levels were comparable in the jugular lymph sac (JLS) and dermal lymphatic vessels (DLV) of control and mutant embryos. Note the presence of autofluorescent blood (white arrows) within the *Chd4$^{fl/fl}$;Lyve1-Cre^{+}* lymphatic vessels. n=3 embryos per genotype. Scale bars: 100µm (A,B); 50µm (C,D). JLS=jugular lymph sac, JV=jugular vein, DLV=dermal lymphatic vessel.

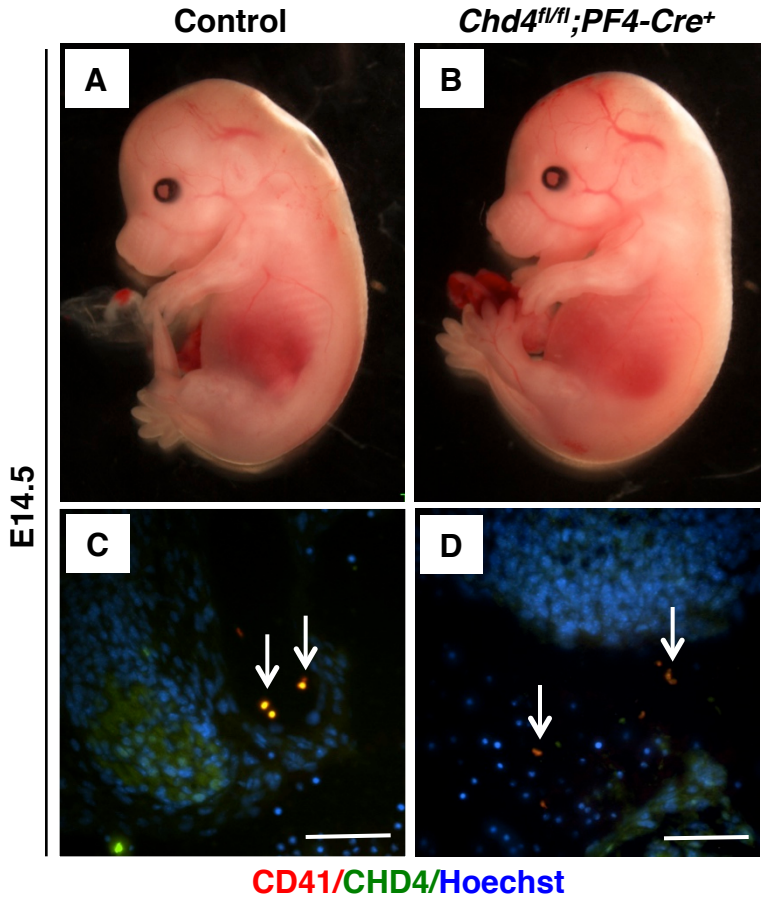

Supplemental Figure 3. *Chd4$^{fl/fl}$;PF4-Cre^{+}* mutant embryos display no overt lymphatic development defects. (A and B): Littermate control **(A)** and *Chd4$^{fl/+}$;PF4-Cre^{+}* **(B)** embryos were dissected and photographed at the same magnification at E14.5. Mutants displayed no evidence of edema or the superficial blood-filled vessels seen in *Chd4$^{fl/fl}$;VE-Cadherin-Cre^{+}* and *Chd4$^{fl/fl}$;Lyve1-Cre^{+}* embryos at this stage (see Figure 1). **(C and D):** Sections from E14.5 control **(C)** and *Chd4$^{fl/fl}$;PF4-Cre^{+}* **(D)** embryos were immunostained for the platelet marker CD41 (red) and for CHD4 (green) and were counterstained with Hoechst (blue) to assess *Chd4* excision efficiency in platelets (white arrows). n=3 embryos per genotype for A and B. n=2 embryos per genotype for C and D. Scale bars: 50μm.

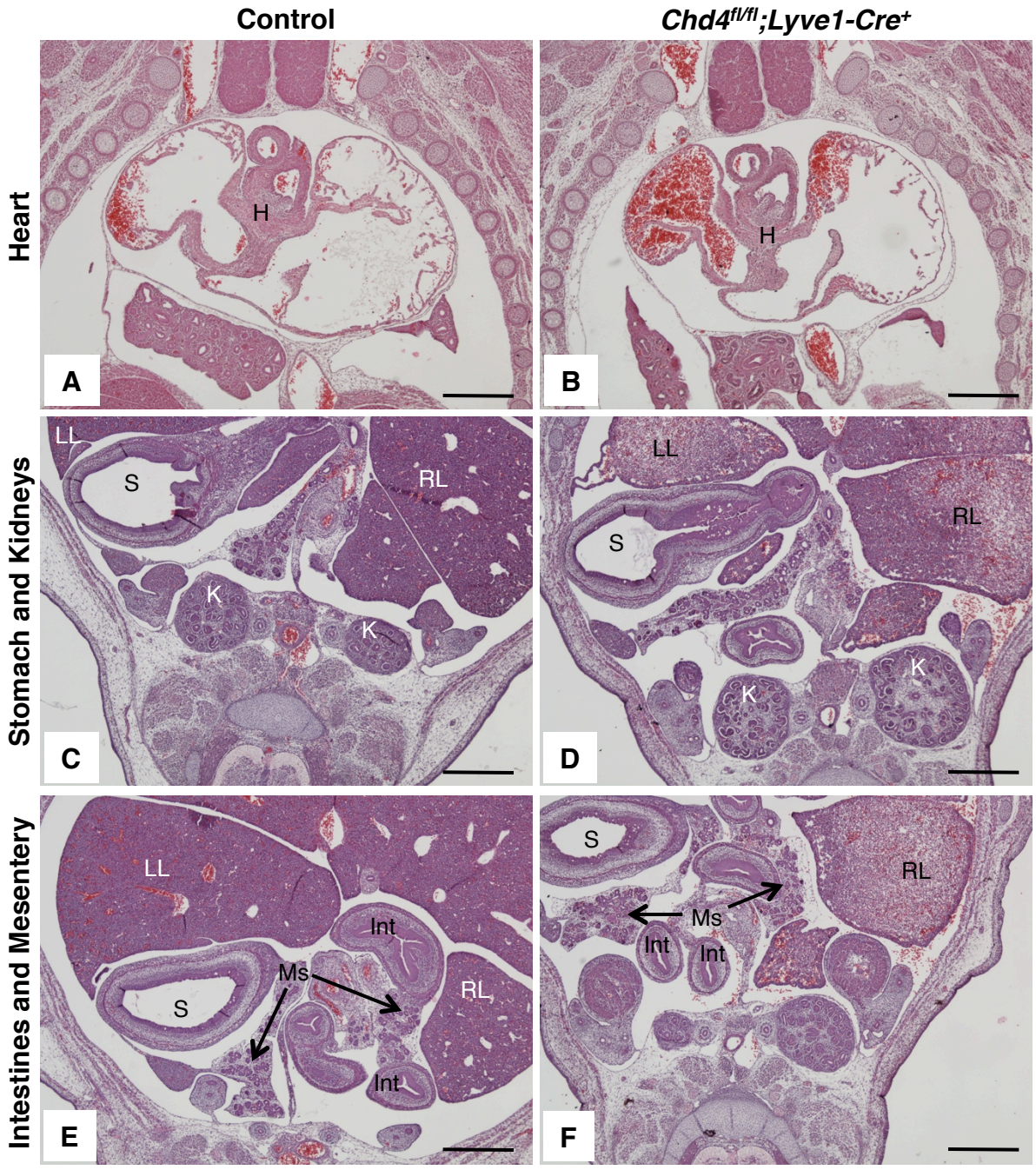

Supplemental Figure 4. *Chd4$^{fl/fl}$;Lyve1-Cre^{+}* mutant embryos have structurally normal hearts, kidneys, stomachs, mesenteries, and intestines. Sections from E14.5 littermate control and *Chd4$^{fl/fl}$;Lyve1-Cre^{+}* embryos were H&E stained to evaluate the morphology of various tissues. n=3 embryos per genotype. Scale bars: 500µm. H=heart, LL=left liver lobe, RL=right liver lobe, K=kidney, Ms=mesentery, S=stomach, Int=intestines.

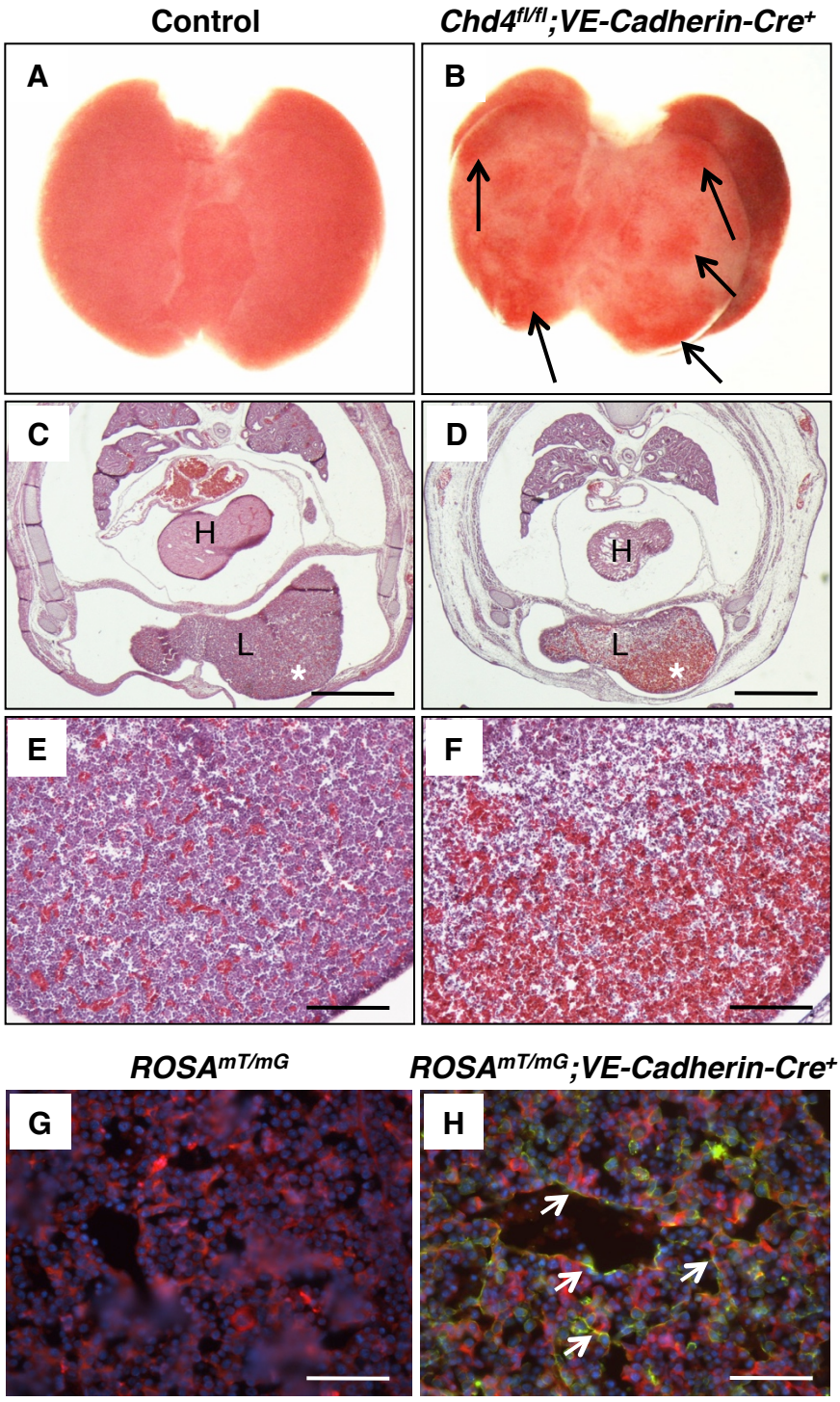

Supplemental Figure 5. Liver hemorrhage is evident in *Chd4$^{fl/fl}$;VE-Cadherin-Cre^{+}* embryos. (A and B): Livers were dissected from E14.5 littermate control **(A)** and *Chd4$^{fl/fl}$;VE-Cadherin-Cre^{+}* **(B)** embryos and photographed. Hemorrhage (black arrows) was grossly evident in the mutant livers. **(C-F):** Control **(C and E)** and *Chd4$^{fl/fl}$;VE-Cadherin-Cre^{+}* **(D and F)** embryos were sectioned and stained with H&E. Hemorrhage was evident in the mutant livers, particularly at the periphery. **E** and **F** depict magnified views of the regions marked with the white asterisks in **C** and **D**, respectively. **(G and H):** To assess the recombinase activity of *VE-Cadherin-Cre* in embryonic livers, E14.5 *ROSA$^{mT/mG}$* **(G)** and *ROSA$^{mT/mG}$;VE-Cadherin-Cre^{+}* **(H)** livers were sectioned and imaged. *ROSA$^{mT/mG}$;VE-Cadherin-Cre^{+}* livers displayed robust Cre activity around blood vessels (green; arrows). n=3 embryos per genotype for A-F. n=2 embryos per genotype for G and H. Scale bars: 500µm (C and D); 100µm (E and F); 50µm (G and H). H=heart, L=liver.

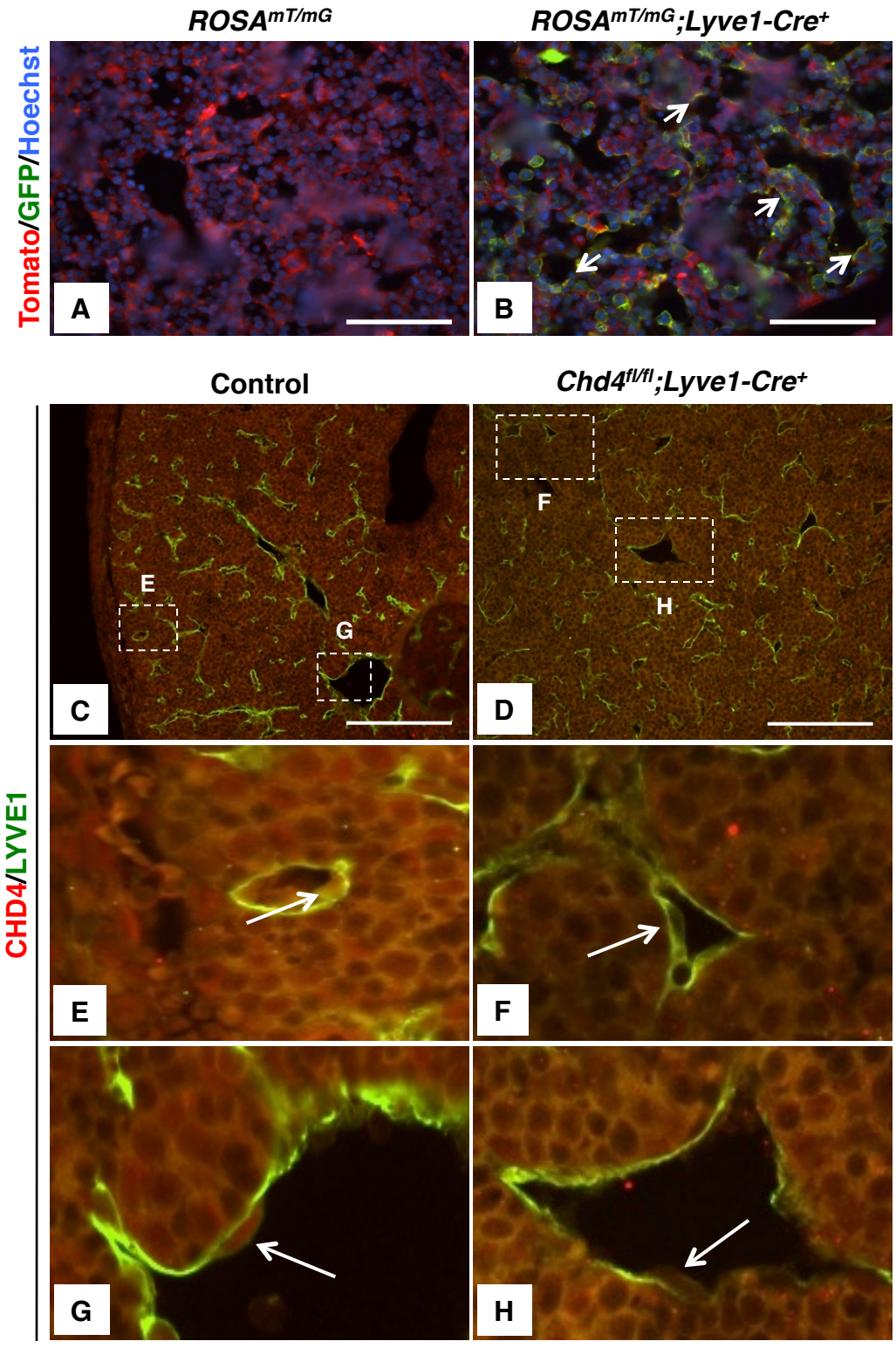

Supplemental Figure 6. *Chd4* is excised in LYVE1⁺ liver blood endothelial cells. (A and B): To assess the recombinase activity of *Lyve1-Cre* in embryonic livers, E14.5 *ROSA*$^{mT/mG}$ **(A)** and *ROSA*$^{mT/mG}$*;Lyve1-Cre*$^{+}$ **(B)** livers were sectioned and imaged. *ROSA*$^{mT/mG}$*;Lyve1-Cre*$^{+}$ livers displayed robust Cre activity around blood vessels (green; arrows). **(C-H):** Sections of livers from E13.5 littermate control **(C, E, and G)** and *Chd4*$^{fl/fl}$*;Lyve1-Cre*$^{+}$ **(D, F, and H)** embryos were immunostained for CHD4 (red) and LYVE1 (green) to assess CHD4 expression in endothelial cells (white arrows) lining blood vessels. **E-H** are magnified images of regions indicated by dotted boxes. n=2 embryos per genotype for A and B. n=3 embryos per genotype for C-H. Scale bars: 50µm (A and B); 200µm (C and D).

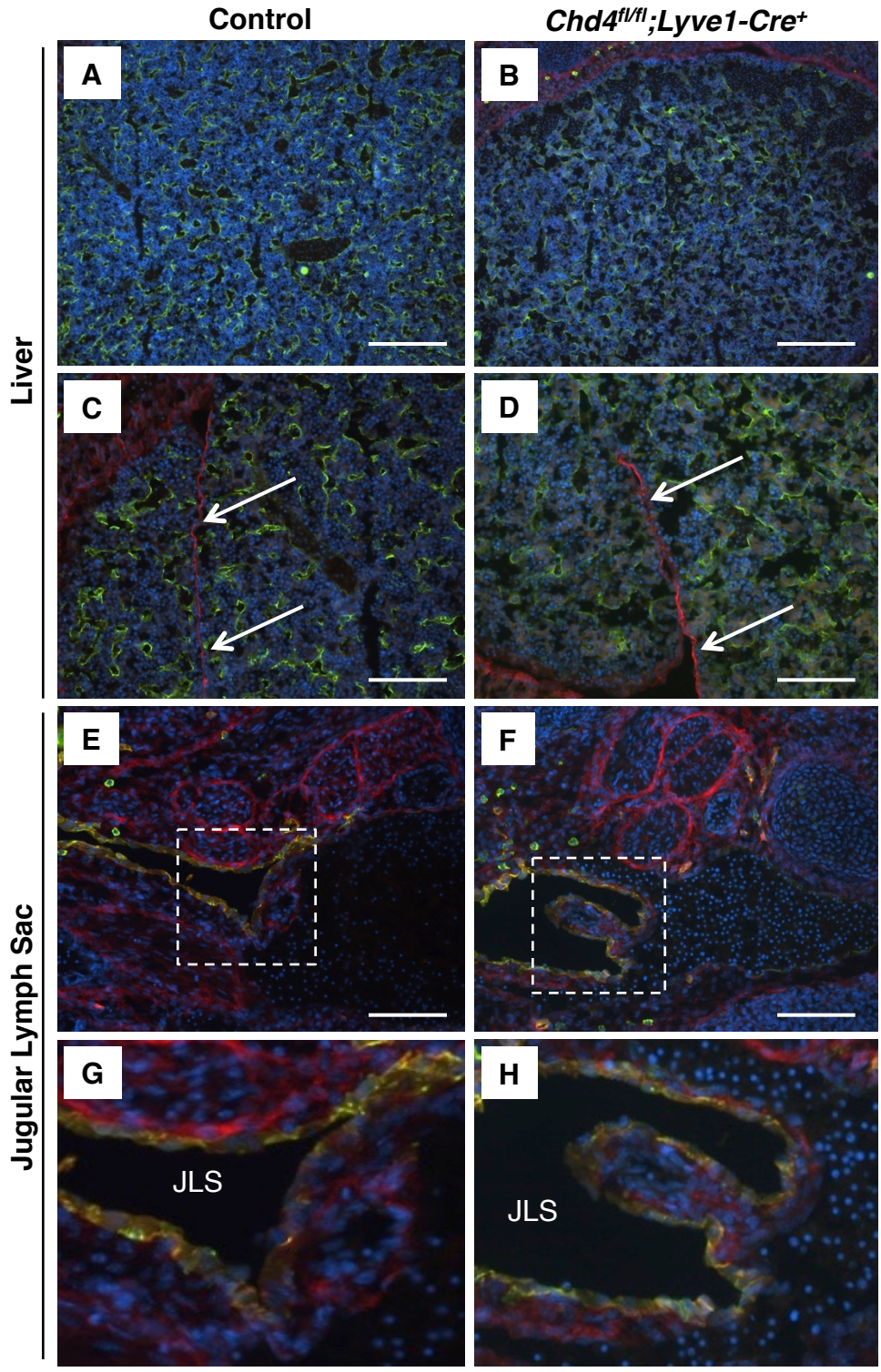

Supplemental Figure 7. Podoplanin is not expressed in E14.5 liver vasculature. Sections from E14.5 littermate control and *Chd4$^{fl/fl}$;Lyve1-Cre^{+}* embryos were immunostained for the LEC marker podoplanin (PDPN) to assess the abundance of liver lymphatics. No PDPN was seen in liver vasculature or hepatocytes **(A and B),** but PDPN was readily detectable in mesothelial cells lining the liver **(C and D)** and in LECs lining the jugular lymph sac **(E-H)**. **G and H** are magnified images of the dotted boxes marked in **E** and **F**, respectively. n=3 embryos per genotype. Scale bars: 200µm (A,B);100µm (C-F). JLS=jugular lymph sac

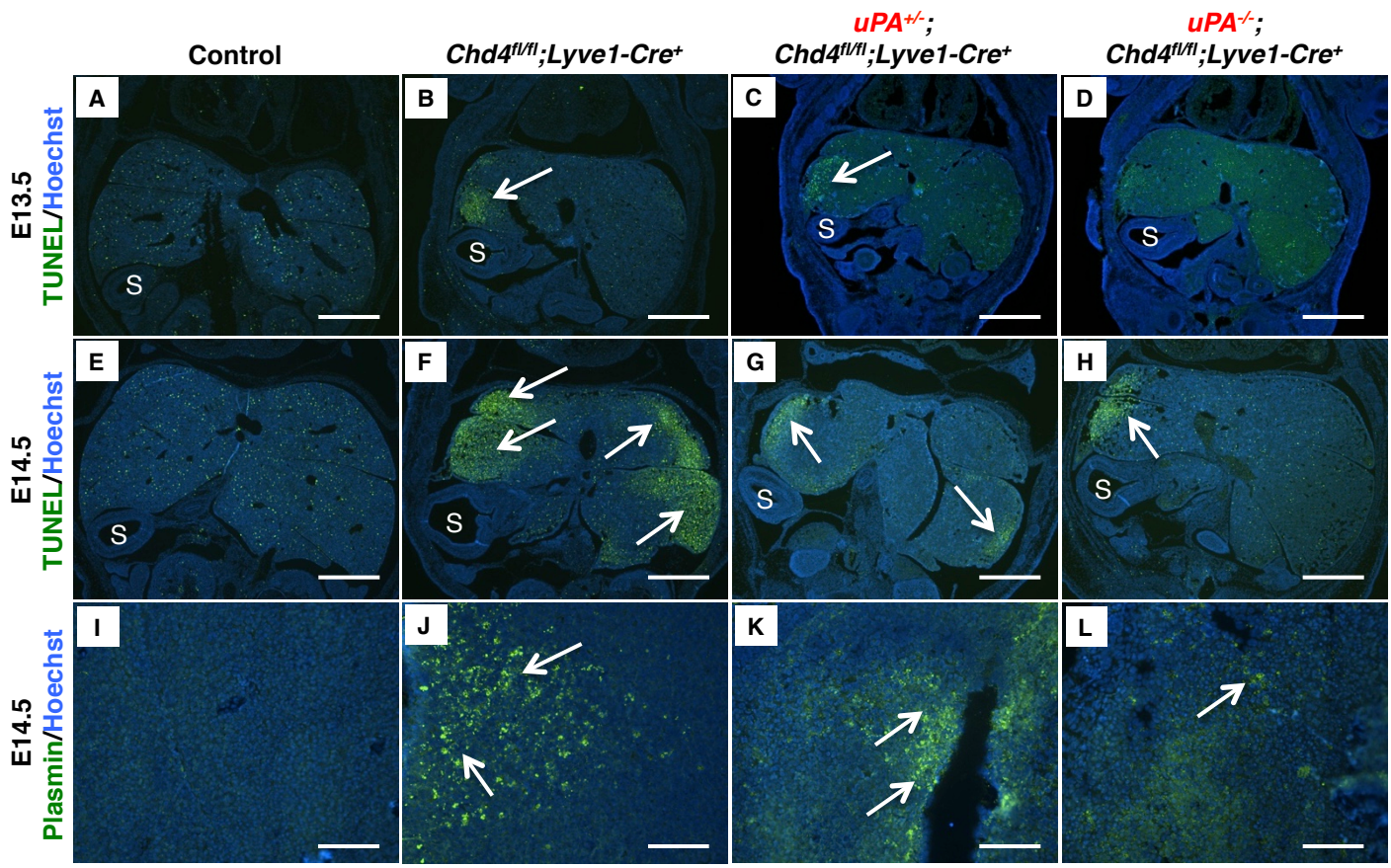

Supplemental Figure 8. Elevated plasmin activity and cell death are not completely eliminated in the left lobes of *Chd4$^{fl/fl}$;Lyve1-Cre^{+}* livers with reduced *uPA*. **(A-H):** TUNEL staining was used to assess cell death in control and mutant embryonic livers. E13.5 *Chd4$^{fl/fl}$;Lyve1-Cre^{+}* livers had increased TUNEL staining primarily concentrated in the left lobe above the stomach **(B, white arrow)**, which was dampened by *uPA* reduction **(C and D)**. By E14.5, TUNEL positive cells were more widespread in *Chd4$^{fl/fl}$;Lyve1-Cre^{+}* liver sections **(F)** and were reduced by *uPA* deletion but still detectable, particularly in the left lobe **(G and H)**. In situ zymography at E14.5 revealed elevated plasmin activity in *Chd4$^{fl/fl}$;Lyve1-Cre^{+}* liver sections **(J);** *uPA* deletion dampened but did not eliminate the plasmin activity **(K and L)**. Scale bars: 500µm (A-H); 100µm (I-J). n=3 embryos per genotype for A-J. n=3 embryos per genotype for K and L. S=stomach.

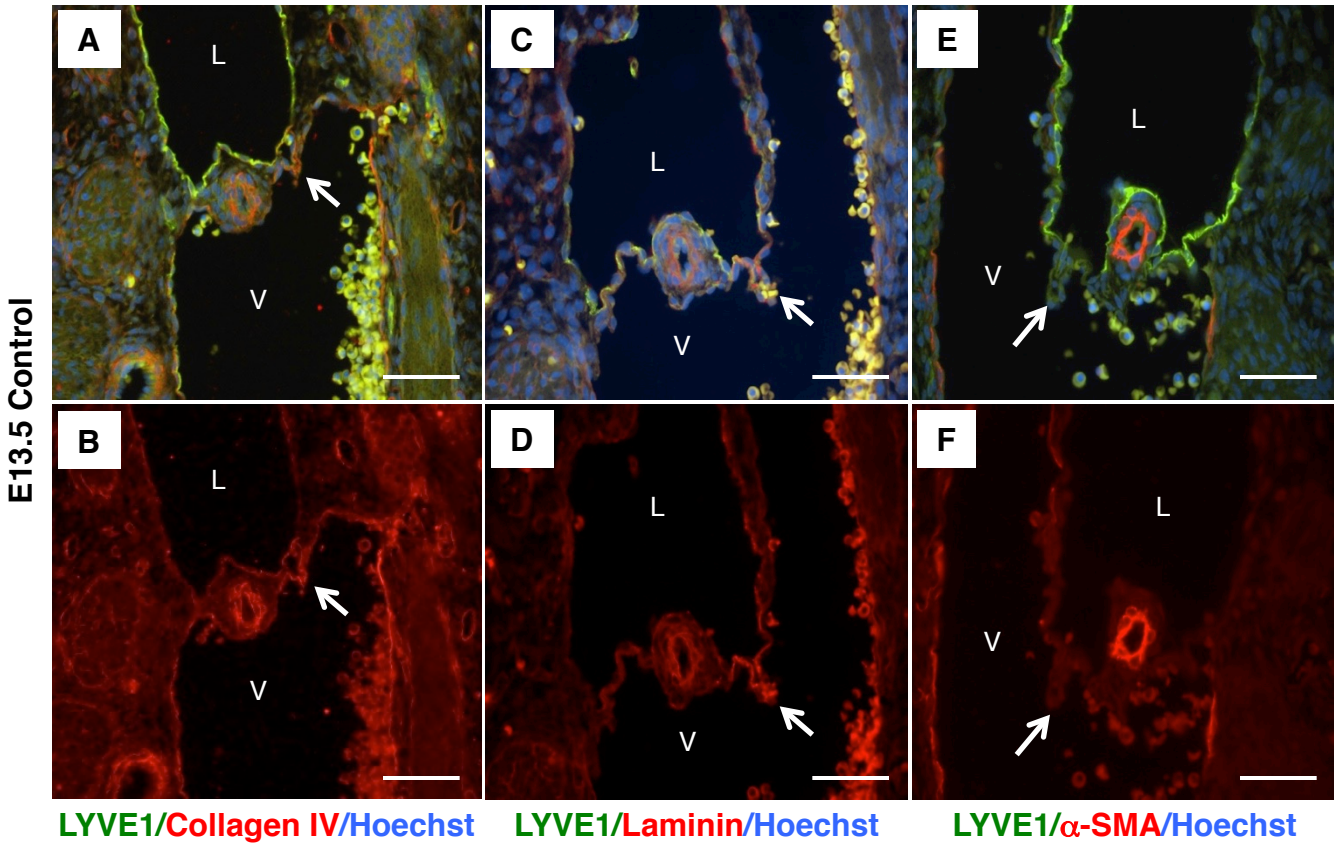

Supplemental Figure 9. LV valves do not express robust extracellular matrix markers at E13.5. Immunostaining was performed to detect expression of the extracellular matrix markers collagen IV (**A and B**, red) and laminin (**C and D**, red) at the LV valves (white arrows) of E13.5 control embryos. Immunostaining was likewise performed for the vascular smooth muscle cell marker α-SMA (**E and F**, red), which is typically seen on mature matrix-secreting cells. None of these markers were robustly or consistently detectable at the LV valves during this stage of development. Panels B, D, and F represent single-color channels of the images shown in A, C, and E, respectively. Scale bars: 50μm for A-F. n=3 embryos each for collagen IV, laminin, and α-SMA. L=jugular lymph sac; V=jugular vein.

Supplemental Table 1

Live offspring at weaning from *Chd4*$^{fl/fl}$ x *Chd4*$^{fl/+}$*;PF4-Cre*$^{+}$ crosses[A]

Genotype	Observed Offspring	Expected Offspring
Chd4$^{fl/+}$	24	16.5
Chd4$^{fl/+}$*;PF4-Cre*$^{+}$	17	16.5
Chd4$^{fl/fl}$	12	16.5
Chd4$^{fl/fl}$*;PF4-Cre*$^{+}$	13	16.5

[A]Ten litters generated from *Chd4*$^{fl/fl}$ females and *Chd4*$^{fl/+}$*;PF4-Cre*$^{+}$ males were genotyped.

Supplemental Table 2

Live offspring at weaning from *uPA*$^{+/-}$;*Chd4*$^{fl/fl}$ x *uPA*$^{+/-}$;*Chd4*$^{fl/+}$;*VE-Cadherin-Cre*$^{+}$ crosses[A]

Genotype	Observed Offspring: Number (%)	Expected Offspring: Number (%)
Chd4$^{fl/+}$	1 (2%)	4 (6.25%)
Chd4$^{fl/+}$;*Lyve1-Cre*$^{+}$	2 (3%)	4 (6.25%)
uPA$^{+/-}$;*Chd4*$^{fl/+}$	16 (25%)	8 (12.5%)
uPA$^{+/-}$;*Chd4*$^{fl/+}$;*Lyve1-Cre*$^{+}$	9 (14%)	8 (12.5%)
uPA$^{-/-}$;*Chd4*$^{fl/+}$	11 (17%)	4 (6.25%)
uPA$^{-/-}$;*Chd4*$^{fl/+}$;*Lyve1-Cre*$^{+}$	7 (11%)	4 (6.25%)
Chd4$^{fl/fl}$	3 (5%)	4 (6.25%)
Chd4$^{fl/fl}$;*Lyve1-Cre*$^{+}$	0 (0%)	4 (6.25%)
uPA$^{+/-}$;*Chd4*$^{fl/fl}$	7 (11%)	8 (12.5%)
uPA$^{+/-}$;*Chd4*$^{fl/fl}$;*Lyve1-Cre*$^{+}$	0 (0%)	8 (12.5%)
uPA$^{-/-}$;*Chd4*$^{fl/fl}$	8 (12%)	4 (6.25%)
uPA$^{-/-}$;*Chd4*$^{fl/fl}$;*Lyve1-Cre*$^{+}$	0 (0%)	4 (6.25%)

[A]Twelve litters generated from *uPA*$^{+/-}$;*Chd4*$^{fl/fl}$ females and *uPA*$^{+/-}$;*Chd4*$^{fl/+}$;*VE-Cadherin-Cre*$^{+}$ males were genotyped.